

OPTIMIZATION OF COMPUTATIONAL SNOW AVALANCHE SIMULATION TOOLS

Jan-Thomas Fischer^{1*}, Andreas Kofler¹, Wolfgang Fellin², Matthias Granig³, Karl Kleemayr¹

¹ Austrian Research and Centre for Forests - BFW, Department of Natural Hazards, Innsbruck, Austria

² University of Innsbruck, Institute of Infrastructure, Division of Geotechnical and Tunnel Engineering

³ Snow and Avalanche Center, Avalanche and Torrent Control - WLV, Innsbruck, Austria

ABSTRACT: Snow avalanche simulation tools are used for hazard estimations and protection planning. Initial conditions and flow model parameters have to be chosen carefully in order to gain meaningful simulation results. A depth averaged flow model is used for this investigation, where simple entrainment and friction relations are implemented in the SamosAT simulation software. The employed mass balance relation allows for the full range of entrainment mechanisms, from frontal plowing to gradual erosion. The initial snow reservoir distribution for release and entrainment is estimated by measurement and empirical observation for the entire mountain. Flow model parameters for the entrainment model and the Voellmy friction relation are systematically optimized by back calculating a documented event. The simulation results are analyzed in three-dimensional terrain with the help of a transformation into an avalanche path dependent coordinate system. Six different optimization variables are scrutinized, related to runout, affected area, velocity, deposition depth and mass growth due to entrainment. The optimization method explicitly takes the uncertainties associated with the observational variables into account. To cover the entire physically relevant parameter range a large number (10^4) of random flow model parameter combinations and their corresponding simulation runs are investigated. This yields posterior parameter distributions representing optimal parameter combinations, which are of fundamental interest for engineers and scientists. We demonstrate how the proposed systematic simulation analysis contributes to an objective parameter calibration and optimization.

KEYWORDS: snow avalanche, computational avalanche dynamics, simulation optimization.

1. INTRODUCTION

Snow avalanche simulation tools are used for hazard estimations and protection planning. Initial conditions and flow model parameters have to be chosen carefully in order to gain meaningful simulation results. Some parameters of the numerical models are more conceptual than physical and have to be determined solving an inverse problem, matching simulation results to field data. Unfortunately quality and availability of field data is generally poor. Furthermore simulations in 3d terrain include large amounts of result data and need adequate evaluation methods. Most studies on avalanche simulation models are based on multi parameter models, but have been optimized for a single optimization variable, namely the avalanche runout. A multivariate optimization method taking into account simulation results in 3d terrain is in great demand.

The aim of the presented work is to employ a method that provides the possibility to optimize multiple model parameters employing a multivariate evaluation of simulation results.

To do so, a simple well-known three parametric flow model including entrainment is implemented in the snow avalanche simulation software SamosAT (**S**now **A**valanche **MO**delling and **S**imulation - **A**dvanced **T**echnology, Zwinger et al., 2003; Sampl and Zwinger, 2004). A large number of simulation runs is performed and the results are analyzed in an avalanche path dependent coordinate system (Fischer, 2013). The main results are parameter distributions for three flow model parameters, that can be utilized as base for future guidelines.

2. AVALANCHE EVENT

Observations on extreme events are important to define simulation input and optimization data, but quality and quantity of extreme avalanche observations is often limited due restricted accessibility (weather, safety, ...). If no field data is available, empirical laws may also provide valuable data for the optimization variables.

* *Corresponding author address:* Jan-Thomas Fischer
Austrian Research and Centre for Forests - BFW,
Department of Natural Hazards,
A-6020 Innsbruck, Austria; Tel.: +43-512 573933 5102
email: jt.fischer@uibk.ac.at



Figure 1: Destroyed houses and infrastructure in the runout area. Picture WLV.

The investigated extreme event is the Wolfsgruben avalanche; on the 13th of March 1988 a catastrophic avalanche struck the village and led to severe loss of life and property (three houses and nine cars were totally destroyed; several other buildings, about 20 cars and a lot of infrastructure got damaged, see figure 1; several people were killed or hurt). The Wolfsgruben avalanche path starts in a release area of ≈ 20 ha at ≈ 2244 m.a.s.l., follows a gully with a width of about 100 m, and finally reaches the community of St. Anton a. A., Austria (at ≈ 1260 m.a.s.l.).

3. AVALANCHE SIMULATION

3.1 Simulation approach

Up to date simulation software for the dense, most destructive part of snow avalanches is mostly based on two dimensional depth averaged, deterministic flow models (Sampl and Zwinger, 2004; Christen et al., 2010; Mergili et al., 2012), describing the evolution of depth averaged flow velocity $\bar{\mathbf{u}}$ and depth \bar{h} . An essential part of snow avalanche modelling is the appropriate choice of bottom friction and entrainment relation. Here, we stick to the well known Voellmy friction relation for the basal shear stress τ_b , which combines a Coulomb bottom friction with a velocity dependent drag term

$$\tau_b = \sigma_b \mu + \frac{g}{\xi} \bar{\mathbf{u}}^2, \quad (1)$$

with the dimensionless Coulomb friction parameter μ and the turbulent friction coefficient ξ [m s^{-2}] (Voellmy, 1955), and a simple assumption for the entrainment rate

$$\dot{q} = \frac{\tau_b}{e_b} \|\bar{\mathbf{u}}\|, \quad (2)$$

that includes the erosion energy parameter e_b [$\text{m}^2 \text{s}^{-2}$].

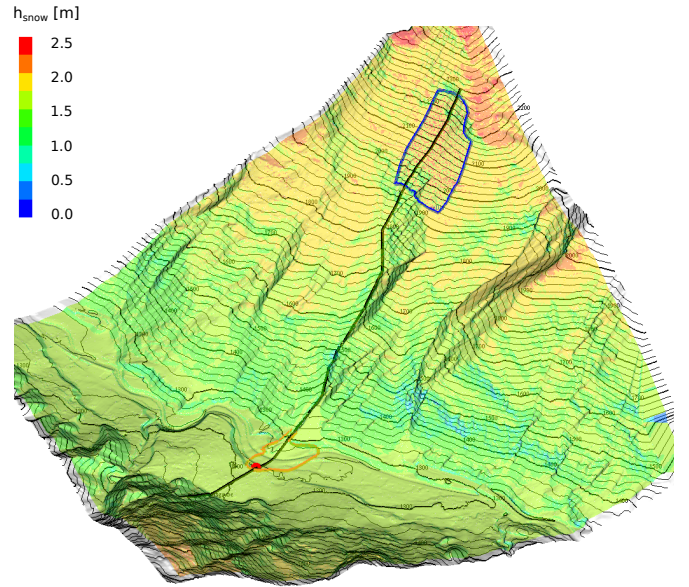


Figure 2: Wolfsgruben avalanche path ($\Delta z = 984$ m). Shown is the snow cover distribution ($h_0 = 1.61$ m, $z_0 = 1289$ m.a.s.l., $\Delta h = 0.08$) and event documentation: central flow line in black, release area (196225 m^2 , with mean slope angle 36.5°) in blue, affected area (64153 m^2 , @ 14.5°) in orange, destroyed house red dot.

3.2 Simulation input

To perform snow avalanche simulations, a parameter set up for the employed flow model and initial conditions have to be defined.

3.2.1 Initial conditions

The mountain surface is represented by a digital elevation model z in a spatial resolution of $5 \text{ m} \times 5 \text{ m}$ to represent the wintery, snow covered surface.

By assuming an initial snow cover distribution

$$h_{snow} = (h_0 + (z - z_0) \Delta h) \cos \theta, \quad (3)$$

the initially released snow mass and the potentially erodible snow are determined in a consistent manner. The precipitation is assumed to be equal at each location, varying with slope θ and altitude z through the snow depth gradient Δh , which is a regional coefficient and varies for different precipitation characteristics (Burkard and Salm, 1992). h_0 is the estimated snow depth measured on flat ground at a reference altitude z_0 . It is often linked to the sum of new snow in 3 days for a certain return period (Burkard and Salm, 1992). Figure 2 shows release area and snow cover distribution, varying with altitude and slope. The total release volume is $V_{\text{release}} = 354617 \text{ m}^3$.

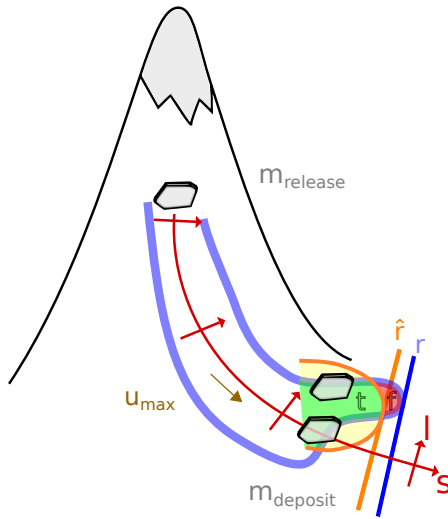


Figure 3: Sketched simulation results (e.g. simulation outline p_{lim} ; blue) and affected area $\hat{A}_{affected}$ (outlined in orange), superimposed with avalanche path domain and new coordinate system along the central flow line (black). run out - r , \hat{r} , matched and exceeded affected area (green, red) - t , f , maximum velocity - u_{max} , average deposition depth - d and mass growth - G .

3.2.2 Flow model parameters $\Theta = \{\mu, \xi, e_b\}$

For each simulation run a set of flow model parameters $\Theta = \{\mu, \xi, e_b\}$ is defined. The appropriate parameter range of each model parameter, i.e. its interval bounds $\Theta_{min}^{prior}, \Theta_{max}^{prior}$ are constrained by physically relevant ranges, results of experimental work or prior model optimization through back calculations. Choosing parameter ranges too small may exclude possible solutions, defining the ranges too large multiplies the computational efforts. Here, the choice of the prior parameter distributions Ω_{Θ}^{prior} includes parameter ranges, based on a scaling analysis of the physically relevant parameter space, i.e. $\mu = [0.1, 0.6]$, $\xi = [400, 15000] \text{ m s}^{-2}$ and $e_b = [0, 75000] \text{ m}^2 \text{ s}^{-2}$, assuming a equal distribution on the entire interval.

3.3 Simulation results

The most important simulation results for the evaluation are the peak values, i.e. maximum values over time, of flow depth h , velocity $|\mathbf{u}|$ and impact pressure $p = \rho |\mathbf{u}|^2$, with $\rho = 200 \text{ kg m}^{-3}$, the density of flowing snow. The simulation results are evaluated in an avalanche path dependent coordinate system, with flow path coordinate s and lateral coordinate l , according to the main flow path shown in figure 2 and a domain width of 500 m (Fischer, 2013).

4. OPTIMIZATION VARIABLES

The optimization variables represent the different categories, that can be accessed through both, observational data and simulation results. In order to perform an objective analysis, a set of six optimization variables $X = \{r, t, f, u_{max}, d, G\}$:

1. run out - r
2. matched affected area (true) - t
3. exceeded affected area (false) - f
4. maximum velocity - u_{max}
5. average deposition depth - d
6. mass growth - G

is defined in terms of either observation and simulation. Observational variables and their associated uncertainty are denoted by $\hat{X} \pm \sigma_{\hat{X}}$, whereas simulation variables by plain X .

4.1 run out - r

For each simulation run, run out r refers to the furthest coordinate s , measured as projected distance in the avalanche path flow direction (Fischer, 2013), where the maximum value of the peak impact pressure in the cross section still exceeds the predefined pressure limit $\max_l p(s, l) > p_{lim}$ (Teich et al., 2013). We set $p_{lim} = 1 \text{ kPa}$, which may be adapted for different hazard mapping guidelines (Johannesson et al., 2009). The observed runout is $\hat{r} = 2219 \text{ m} \pm 50 \text{ m}$.

4.2 relative matched and exceeded affected area - t, f

We assume that peak pressures observed in the avalanche \hat{p} exceed the pressure limit p_{lim} , i.e. $\hat{p} > p_{lim}$ inside the observed affected area. Considering given affected and total area, two independent relations can be specified as:

- true prediction - simulated area t with $p > p_{lim}$ matching observed affected area $\hat{A}_{affected}$
- false prediction - simulation area f with $p > p_{lim}$ exceeding observed affected area $\hat{A}_{affected}$

The observational value for the optimization variable *true prediction* t relative to the affected area $\hat{A}_{affected}$ itself is given by $\hat{t} = 1$ and consequently for the *false prediction* f by $\hat{f} = 0$. The associated uncertainty is estimated relative to the affected area to $\sigma_{\hat{t}, \hat{f}} = 0.1$.

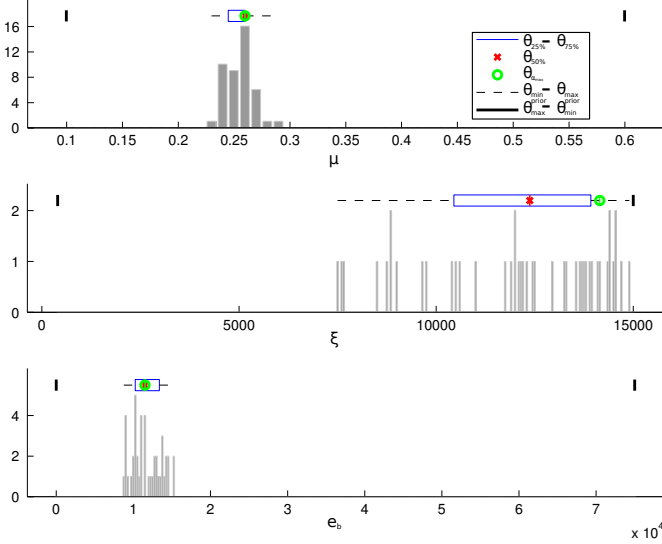


Figure 4: Posterior parameter frequency Ω_{Θ} for simulation runs with $\alpha > \alpha_{\text{lim}}$. The box plot above summarizes some statistical features of the posterior distributions Ω_{Θ} such as the minimum value Θ_{\min} , the 25%, 50% and 75% quantiles $\Theta_{25\%}$, $\Theta_{50\%}$, $\Theta_{75\%}$ and the maximum value Θ_{\max} . To provide a reference to the prior distribution $\Omega_{\Theta}^{\text{prior}}$ the minimum and maximum values $\Theta_{\min}^{\text{prior}}$, $\Theta_{\max}^{\text{prior}}$ are shown.

4.3 maximum velocity - u_{\max}

The maximum velocity u_{\max} is defined for each simulation run by taking the maximum of the peak velocities over the entire simulation domain:

$$u_{\max} = \max_{s,l} \|\bar{\mathbf{u}}\|. \quad (4)$$

The observational maximum velocity along an avalanche path with fall height Δz is estimated by $\hat{u}_{\max} \approx 0.6 \sqrt{g \Delta z}$ (McClung and Schaerer, 2006). For the investigated Wolfsgruben avalanche path the maximum velocity is $\hat{u}_{\max}(\Delta z = 984 \text{ m}) = 58.9 \pm 2.5 \text{ m s}^{-1}$.

4.4 average deposition depth - d

The average deposition depth is defined as observed depth, averaged in the affected area and is directly measured in the field. For the Wolfsgruben avalanche deposition $\hat{d} = 4 \pm 0.5 \text{ m}$ were observed.

For the simulation deposition depths, we take the peak flow depth h and define $d = h \frac{\rho}{\hat{\rho}_{\text{deposit}}}$ ($\hat{\rho}_{\text{deposit}} = 400 \text{ kg m}^{-3}$) averaged in the affected area, taking into account that the employed flow model does not allow for densification or deposition; densification in snow avalanches can reach, comparing released, flowing and deposited snow, a factor of three (Ancey, 2005).

Table 1: Information on the posterior distribution Ω_{Θ} of optimization variables Θ . Listed are minimum and maximum value Θ_{\min} , Θ_{\max} , 25%, 50% and 75% quantiles for each parameter $\Theta_{25\%}$, $\Theta_{50\%}$, $\Theta_{75\%}$ and $\Theta_{\alpha_{\max}}$.

	Θ_{\min}	$\Theta_{25\%}$	$\Theta_{50\%}$	$\Theta_{\alpha_{\max}}$	$\Theta_{75\%}$	Θ_{\max}
μ	0.23	0.24	0.26	0.26	0.26	0.29
ξ [m s^{-2}]	7500	8825	12375	14150	13925	14900
e_b [$\text{m}^2 \text{ s}^{-2}$]	8750	10250	11500	11500	13375	15250

4.5 mass growth - G

The mass growth index G is defined as the ratio of deposited to released mass, describing the increase of flowing avalanche mass due to entrainment with a dimensionless number

$$G = \frac{m_{\text{deposit}}}{m_{\text{release}}}. \quad (5)$$

For the Wolfsgruben avalanche the mass growth is estimated to $\hat{G} = 1.45 \pm 0.1$.

5. OPTIMIZATION

The goal of the proposed optimization is to provide an objective, scalar metric, which describes the correspondence between a single simulation run and the documentation.

For each optimization variable a measure of the correspondence between observation and simulation is introduced as a normalized, Gaussian function \mathcal{N} with mean \hat{X} and variance $\sigma_{\hat{X}}^2$:

$$\alpha_{X(\Theta)} = \frac{\mathcal{N}(X(\Theta) | \hat{X}, \sigma_{\hat{X}}^2)}{\mathcal{N}(\hat{X} | \hat{X}, \sigma_{\hat{X}}^2)}. \quad (6)$$

The obtained value is bounded in the interval $[0, 1]$, where $\alpha_{X(\Theta)} = 0$ indicates negligible agreement and $\alpha_{X(\Theta)} = 1$ optimal correspondence. So we determine the metric $\alpha_{X(\Theta)}$ for each optimization variable $X = \{r, t, f, u_{\max}, d, G\}$, conditional on the choice of the prior parameter set $\Theta = \{\mu, \xi, e_b\}$, summarized in a target function $\alpha(\Theta)$

$$\alpha(\Theta) = \sum_X w_X \alpha_{X(\Theta)}. \quad (7)$$

Thereby is $\sum_X w_X \stackrel{!}{=} 1$, such that $\alpha(\Theta)$ is also bounded by the interval $[0, 1]$. The weighting factors w_X allow to emphasize or reduce the importance of certain optimization variables. So the optimization method can easily be adopted to cases with more or less observational data.

A correspondence limit α_{lim} is used as a selection rule to determine the simulation runs with $\alpha(\Theta) > \alpha_{\text{lim}}$. The related frequency distribution Ω_{Θ} is analyzed for each of

the model parameters $\Theta = \{\mu, \xi, e_b\}$. Of particular interest are statistical features, such as the 25%, 50% (median) and 75% quantiles for each parameter $\Theta_{75\%}$, $\Theta_{50\%}$, $\Theta_{75\%}$, minimum and maximum value Θ_{\min} , Θ_{\max} and the parameter value $\Theta_{\alpha_{\max}}$ that corresponds to the highest simulation-observation correspondence, i.e. $\max \alpha(\Theta)$.

In figure 4 and table 1 the results of the analysis of the posterior parameter distributions Ω_{Θ} for $\Theta = \{\mu, \xi, e_b\}$ applying a correspondence limit $\alpha_{\text{lim}} = 0.64$ are shown. We conclude, that for μ and e_b a clear peak is found, i.e. $\Theta_{25\%}$, $\Theta_{50\%}$, $\Theta_{75\%}$ and $\Theta_{\alpha_{\max}}$ are relatively close, see table 1. For ξ not a peak, but rather a lower boundary is found.

6. CONCLUSIONS

With the presented framework of simulation and optimization, a method is developed, that allows to optimize multiple model parameters using a multivariate evaluation by comparing simulation results with field data, based on an objective, scalar metric.

10^4 simulation runs have been performed with varying parameter sets Θ . Parameter sets with high correspondence have been identified, analyzing simulated and belonging observed optimization variables \hat{X} using the scalar metric $\alpha(X)$. For the given event, the evaluation showed a clear peak for $\mu_{25\%} = 0.24 < \mu < \mu_{75\%} = 0.26$ and $e_{b,25\%} = 8825[\text{m}^2 \text{s}^{-2}] < e_b < e_{b,75\%} = 13925[\text{m}^2 \text{s}^{-2}]$, moreover this coincides with the parameter values of maximum correspondence $\mu_{\alpha_{\max}} = 0.26$ and $e_{b,\alpha_{\max}} = 11500$ highlighting the information value. For ξ a lower bound $\xi > \xi_{\min} = 7500[\text{m s}^{-2}]$, but no peak or upper limit was identified. This means that the optimal value of ξ is some arbitrary value larger than ξ_{\min} . However, for ξ values in this range, the effect of the turbulent friction becomes negligible.

The strength of this optimization concept is the possibility to be adopted to other optimization variables, flow models and their related parameters. For further details on the employed method and its results we refer to the full paper that will be published elsewhere.

ACKNOWLEDGEMENT

This research work was carried out with the financial support of the project CoSiCa (BMLFUW - Federal Ministry of Agriculture, Forestry, Environment and Water Management, WLW - Austrian Service for Torrent and Avalanche Control).

REFERENCES

- Ancey, C., 2005: Monte Carlo calibration of avalanches described as Coulomb fluid flows. *Philosophical Transactions of the Royal Society A: Mathematical, Physical and Engineering Sciences*, **363**, 1529–1550.
- Burkard, A., and B. Salm, 1992: Die Bestimmung der mittleren Anrissmächtigkeit d_0 zur Berechnung von Fliesslawinen. SLF, Davos, Switzerland.
- Christen, M., J. Kowalski, and P. Bartelt, 2010: RAMMS: Numerical simulation of dense snow avalanches in three-dimensional terrain. *Cold Regions Science and Technology*, **63**, 1–14.
- Fischer, J.T., 2013: A novel approach to evaluate and compare computational snow avalanche simulation. *Natural Hazards and Earth System Science*, **13**, 1655–1667.
- Johannesson, T., P. Gauer, P. Issler, and K. Lied, 2009: The design of avalanche protection dams. *Recent practical and theoretical developments European Commission. Directorate General for Research, Brussels, Belgium*.
- McClung, D.M., and P. Schaerer, 2006: *The avalanche handbook*. The Mountaineers Books.
- Mergili, M., K. Schratz, A. Ostermann, and W. Fellin, 2012: Physically-based modelling of granular flows with Open Source GIS. *Natural Hazards and Earth System Sciences*, **12**, 187–200.
- Sampl, P., and T. Zwinger, 2004: Avalanche simulation with SAMOS. *Annals of Glaciology*, **38**, 393–398.
- Teich, M., J.T. Fischer, T. Feistl, P. Bartelt, P. Bebi, M. Christen, and A. Grêt-Regamey, 2013: Evaluation and operationalization of a forest detrainment modeling approach for computational snow avalanche simulation. In: *AGU General Assembly 2013, San Francisco, USA*.
- Voellmy, A., 1955: Über die Zerstörungskraft von Lawinen. *Schweizerische Bauzeitung, Sonderdruck aus dem 73. Jahrgang*, 1–25.
- Zwinger, T., A. Kluwick, and P. Sampl, 2003: Numerical simulation of dry-snow avalanche flow over natural terrain. *Dynamic Response of Granular and Porous Materials under Large and Catastrophic Deformations, Hutter, K. and Kirchner, N., Springer Verlag*, **11**, 161–194.